Journal of Power Sources 218 (2012) 52–55

Contents lists available at SciVerse ScienceDirect

Journal of Power Sources

journal homepage: www.elsevier.com/locate/jpowsour

Short communication

Dissecting anode swelling in commercial lithium-ion batteries

Ningxin Zhang*, Huaqiong Tang

Amperex Technologies Limited, No. 1 West Industrial Road, Song Shan Lake, DongGuan, GuangDong 523808, People's Republic of China

HIGHLIGHTS

- ► Anode with pristine and lithiated graphite is formed via selective shielding cathode.
- ► Microscopic lattice constants of pristine and lithiated graphite are analyzed via XRD.
- ► Macroscopic anode thickness at pristine and lithiated graphite parts are measured.
- ► Anode swelling is directly correlated to lattice expansion at different SOC.
- ► Mechanism of anode swelling is analyzed.

ARTICLE INFO

Article history:
Received 19 March 2012
Received in revised form
2 June 2012
Accepted 21 June 2012
Available online 3 July 2012

Keywords:
Lithium-ion battery
X-ray diffraction
Lithium-ion intercalation
Lattice expansion
Anode swelling

ABSTRACT

An innovative method is applied to investigate anode swelling during electrochemical processes in commercial lithium-ion batteries. Cathode surface is partially covered with a piece of paste to block the transportation of lithium ion from active material during charging/discharging, and the corresponding part on the anode film shows no formation of Li-graphite compounds during different electrochemical processes, which is confirmed by XRD analysis. The increases of anode thickness within and outside lithiated zone are measured, and defined as electrochemical swelling and physical swelling respectively. The microscopic lattice expansion of graphite due to lithiation process correlates to mesoscopic electrochemical swelling synchronically, while physical swelling tends to decrease steadily with time. The relationship among the microscopic stress due to lithium-ion intercalation, the mesoscopic stress resulting in anode swelling, and the macroscopic rippling of pouch cell after a large number of cycle test, is analyzed and correlated in terms of stress evolution across different scales, and suggestions for solving anode swelling are provided.

1. Introduction

With the increasing requirement of high capacity lithium-ion batteries (LIB) from consuming electronics, active materials with high energy density are being developed such as NCM [1–4] and Li-rich materials [5] as cathodes, and Si–C alloy for anodes [6,7].

Despite this pursuit of high energy density materials, manufacturing process optimization for controlling the thickness increase of the commercial pouch cells is an alternative solution to save more space for active materials. Currently, a thickness increase of 6–20% after high temperature storage/cycling test is usually measured in the commercial pouch cells, the deterioration of cell performance such as capacity diving is often observed in the thickened pouch cells which is ascribed to the formation of microcracks among graphite particles leading to the increase of the electrical impedance, and the shortage of electrolyte due to the growth of gap/void between anode and cathode films where much electrolyte is required to fill.

It's well accepted that the intercalation of lithium ion into graphite results in the lattice expansion of graphite in terms of the formation of Li–C compounds including LiC_{72}, LiC_{36}, LiC_{24}, LiC_{12}, and LiC_6 [8] gradually, and the associated microscopic stress is the intrinsic driving force of anode swelling. J. Christensen and J. Newman have simulated the stress distribution and its influence on graphite particles after Li ion intercalation [9,10], S. J. Harris reported that mesospores in porous electrode can modify the associated stress in anode film during Li ion transportation and diffusion in charging and discharging processes [11]. However, to suppress the thickness increase of the commercial pouch cells, the intrinsic correlation between Li ion intercalation and anode swelling must be revealed. Moreover, it is reported recently that a serious anode swelling is encountered during the commercialization of Si–C alloy, where a huge volumetric expansion of ~400% is generated!

* Corresponding author.
E-mail address: zhangnx@atlbattery.com (N. Zhang).

0378-7753/$ – see front matter © 2012 Elsevier B.V. All rights reserved.
http://dx.doi.org/10.1016/j.jpowsour.2012.06.071

How the microscopic lattice expanding affects the measurable anode swelling, and contributes to the visible thickening/rippling of the commercial pouch cell is not clear till now. One of the reasons is that it is difficult to bridge variation of lattice constant to that of anode thickness directly.

Here, we report an innovative method to investigate the influence of microscopic Li ion intercalation on anode swelling.

2. Experimental

A batch of Jelly-Rolls of ATL's commercial LIB was prepared. The active materials of cathode and anode are $LiCoO_2$ and artificial graphite respectively, both made by local manufacturers. Each Jelly-Roll was firstly disassembled and a square green film resistant to electrolyte with a dimension of 2 cm × 2 cm × 20 μm was pasted to the central position of the cathode film in the 5th layer of a 10-layer Jelly-Roll as shown in Fig. 1, and no treatment was applied to the opposite anode film. The winded Jelly-Rolls were injected with electrolyte in vacuum, packaged, and followed by formation, charging and discharging to a series of voltage.

After the designed electrochemical processes, those polymer cells were disassembled in a drying room with the controlled humidity less than 2% (RH). The thickness in the central part and surrounding part of each anode film right opposite to the partially covered cathode was measured immediately with a micrometer with the resolution of 1 μm to avoid any side reactions between anode film and moisture in air. To assure the accuracy of the thickness measurement, 5–6 positions were measured and each measurement was repeated for 8–10 times.

For the microstructure analysis, those anode films were cut into a size of 4 mm × 12 mm and sealed with a transparent glue film with a thickness of 50 μm tightly in the drying room. Those samples were then delivered for XRD (Model: Rigaku, Cu as target) analysis within minutes. The strongest diffraction peaks corresponding to the (002) plane in the XRD patterns were calculated to get the lattice constant d based on Bragger's equation on diffraction in a single phase. In the case of mixed phases where the cell was charged to 4.2 V with the co-existence of LiC_{12} and LiC_6 phases, the areas of the strongest diffraction peaks of each individual phase were calculated as A_1 (LiC_{12}) and A_2 (LiC_6) respectively, based on the rough assumption of an isosceles triangle of the diffraction peak, and the lattice constants were calculated as d_1 (LiC_{12}) and d_2 (LiC_6), then the area weighted lattice constant of the mixed phases was defined as $(A_1{}^*d_1 + A_2{}^*d_2)/(A_1 + A_2)$. The lattice expansion was then calculated as $(d' - d^0)/d^0 \times 100\%$, where d' and d^0 were the lattice constants of lithiated phase and pristine graphite respectively.

The cross section of anode film was investigated with SEM (Joel 6301F) after quenched in liquid nitrogen. For the non-destructive investigation of Jelly-Rolls in the pouch cell, one seriously rippled cell after 2000 cycling test (parameter: 0.7C charged to 4.2 V/0.5C discharged to 3.0 V) was scanned with a Micro-CT (Shimadzu, Japan).

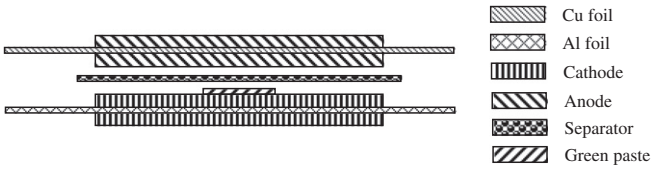

Fig. 1. Schematics of shielding the cathode.

3. Results and discussions

3.1. Anode film shielded from lithium-ion intercalation

Fig. 2a shows the anode film opposite to the partially covered cathode in a pouch cell charged to 4.2 V, where the central part of the anode (defined as shielded area in the following text) looks black as pristine graphite without Li ion intercalation, and the surrounding part shows golden color which is the characteristic of the saturated Li–C compound. This result is confirmed by the X-ray diffraction patterns shown in Fig. 3, where a series of XRD patterns are compared for the different anode films: in the shielded part of anode film which was charged to 4.2 V (labeled as shielded); after formation at 3.4 V (labeled as Form. at 3.4 V); charged to 3.9 V (labeled as CH to 3.9 V); charged to 4.2 V (labeled as CH to 4.2 V); discharged to 3.9 V after charged to 4.2 V (labeled as DC to 3.9 V); discharged to 3.4 V after charged to 4.2 V (labeled as DC to 3.4 V). In Fig. 3, the characteristic diffraction peak of graphite remains in the shielded part of anode film, while in its neighboring area, the characteristic peaks of LiC_{12} and LiC_6 are detected in the same piece of the anode film, and that of LiC_{12} detected for cell charged/discharged to 3.9 V. Those results imply that the pristine graphite does co-exist with the fully lithiated graphite in the same anode sheet under 100% state of charging (SOC), and the thickness variation of the central pristine graphite should not be ascribed to the Li ion intercalation.

This result confirms the feasibility of modulating the transportation of lithium ion between cathode and anode in the pouch cells during the electrochemical process via the physical blocking on its transporting path. It is therefore, an effective method to distinguish the influences associated with the Li ion intercalation on the anode film from any other physical process irrelevant to or not induced by the transportation and diffusion of Li ion.

3.2. Anode swelling due to the electrochemical reaction

The intercalation of lithium ion into graphite is believed to be the essential driving force toward anode swelling during the electrochemical process. It is difficult to quantify the influence of lithium-ion intercalation on the anode swelling process independently since anode film is consisted of graphite particles, binders, conductive additives, and pores formed among them, and the lattice expansion of graphite due to the lithium-ion intercalation is accompanied with the structural evolution of the binders, and the porous configuration in anode film. As mentioned above, with this innovative method it is able to clearly isolate the influence of the lithiation process on anode swelling from other non-electrochemical process.

Fig. 2b describes the definition of associated parameters on dividing the anode swelling into two categories: electrochemical process induced anode swelling and physical swelling due to volumetric evolution of polymers such as binders and dispersive agents after long time soaking in electrolyte. The thicknesses of the anode film before being winded into Jelly-Roll, in the shielded and lithiated part after electrochemical process are defined as T_0, T_1 and T_2, respectively; the thickness of Cu foil is 8 μm. The physical swelling is defined as the ratio between $(T_1 - T_0)$ and T_0, and the electrochemical swelling as the ratio between $(T_2 - T_1)$ and T_1 based on a simple assumption that lithiation and swelling of polymers are two independent processes. Those data can be easily obtained through the basic mathematic calculation among measured data of t_0, t_1, t_2 in Fig. 2b.

The shielded and lithiated parts of anode film are neighbored to each other in mm scale laterally in the anode film and the thickness variation of mass production line is within ±5 μm in ~500 mm, the

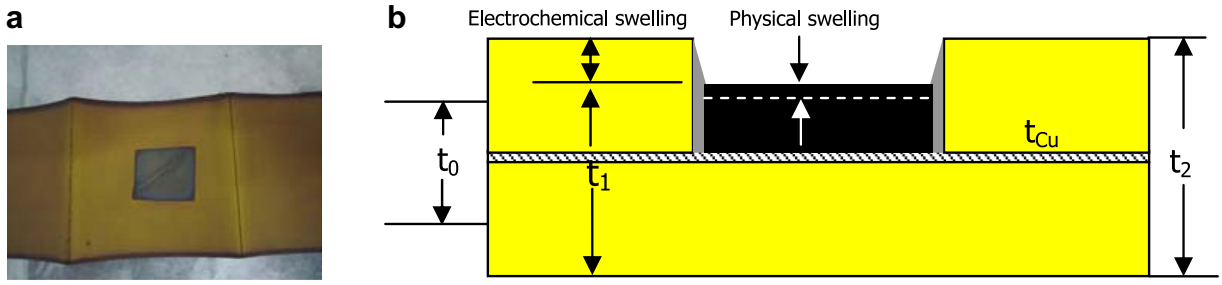

Fig. 2. Anode swelling after full charging. a. Disassembled anode film; b. Schematics of the definition and calculation of the electrochemical and physical swelling.

thickness fluctuation of anode film after calendaring and slitting among different batches in this experiment could be controlled within 1 μm; the measurement is carried out at the same position of each anode film, therefore, it is believed that the accuracy of thickness measurement can be guaranteed.

In Fig. 4a, the anode swelling trend as a function of electrochemical process is plot. As it shows, the lattice expansion is trigged upon Li ion intercalation, and it reaches to 4.7% after the formation of LiC_{12}, and to 7.1% as a peak due to the formation of the mixed LiC_6 and LiC_{12} compounds. The lattice expansion decreases again to 4.7% when discharged to 3.9 V, and to 0 when discharged to 3.4 V.

For the electrochemical swelling, it also shows a reversible trend between charging and discharging: steps from 0% at formation of 3.0 V, reaches a peak of 14.2% when charged to 4.2 V, and decreases to 9.6% after discharged to 3.8 V due to de-intercalation of lithium ion from graphite. The difference between electrochemical swelling and lattice expansion increases to about 6.5% when the cell is charged to 4.2 V, and then keeps unchanged even the cell is discharged to 3.4 V, thus a residual electrochemical swelling of 6.5% remains in the lithiated anode film although no Li–C compound can be detected. The result indicates that the anode film undergoes a structural adjustment accompanied with the lattice expansion of graphite particles, and this adjustment shifts the stacking variation of the graphite particles in anode film permanently, which can not be recovered.

As to the physical swelling as a function of time shown in Fig. 4b, an interesting phenomenon is observed, thus it decreases steadily from 3.0% at formation, to −3.2% corresponding to being discharged to 3.4 V, which might be due to the continuous and consistent structural weakening of polymers after being soaked in electrolyte with a long time, which can be attributed to the aging/relaxation of chain in the structure of polymers. It seems that there is no direct correlation between electrochemical swelling and physical swelling.

Judging from the curve of lattice expansion, the lithiation and de-lithiation processes are reversible, while the associated mechanical or structural change in anode film is irreversible.

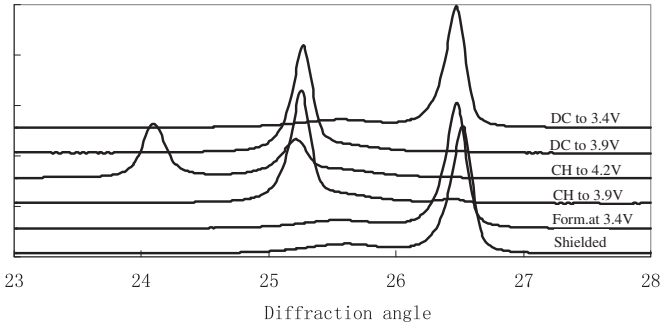

Fig. 3. XRD patterns of the shielded and lithiated anode films.

3.3. Swelling mechanism

To unveil the mechanism standing behind the thickening/rippling phenomenon of the commercial pouch cell, tracing the stress evolution through the microscopic, mesoscopic, and macroscopic scales will give a more clear view.

Fig. 5 shows three typical schematics or photos for dissecting swelling mechanism in different scales. Fig. 5a illustrates the microscopic lattice expansion of graphite covered with SEI film after lithiation process, where the expansion of the individual graphite domain/particle points vertically to the graphene plane as indicated by arrows, but for the anode film consisted of randomly aligned graphite particles, the overall expansion direction in the lithiated anode film is anisotropic.

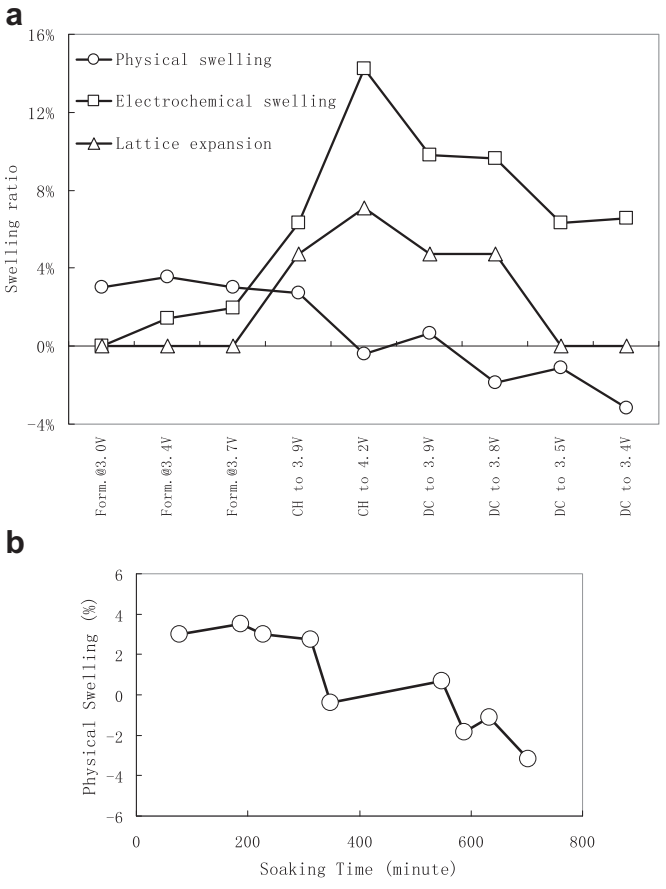

Fig. 4. Trends of the anode swelling as a function of electrochemical process. a. Correlation of the lattice expansion, electrochemical swelling and physical swelling; b. Physical swelling as a function of soaking time in electrolyte.

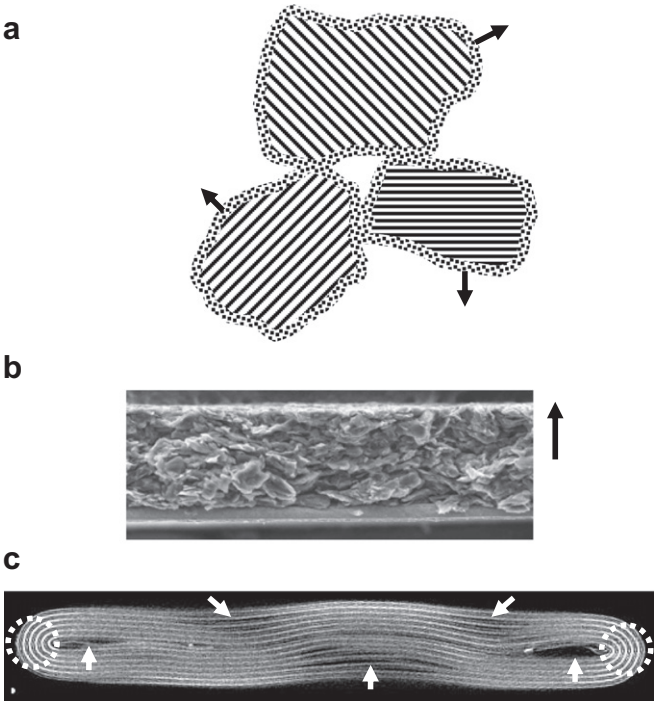

Fig. 5. Mechanism analysis of anode swelling. a. Schematics of the graphite lattice expansion; b. SEM microscopy of the cross section of an anode film; c. Micro-CT view of the cross section of a buckled Jelly-Roll.

Fig. 5b shows the cross section view of an anode film after calendaring process, part of those graphite particles is aligned parallel to Cu foil. Usually, graphite particles are adhered to the Cu foil with binders such as SBR (Styrene-Butadiene Binder), therefore the interface between Cu foil and graphite film doesn't undertake relative movement during the swelling process except some extreme condition where anode graphite may detach from the Cu foil. Graphite particles are pressed and stacked closely to each other, lateral expansion is negligible, the isotropic distribution of the volumetric expansion of individual graphite particle in Fig. 5a is then shaped to a unique swelling perpendicular to the anode film as shown by arrow. The expansion/swelling is simultaneously amplified from the isotropic value of ~7% in graphite particles to the anisotropic one of ~14% as shown in Fig. 4a! The difference between lattice expansion and anode swelling may change in cases of graphite with different particle size distribution, pressing density as well as concentration of polymers in the anode film.

To suppress anode swelling induced by lattice expansion, the configuration of anode film can be optimized through a combination of particles with different size, stronger binders, or optimized distribution of pore configuration to release stress accumulated in anode swelling process.

Fig. 5c shows a micro-CT image along the cross section of a rippled pouch cell, where the two winding edges of Jelly-Roll are fixed by the packing foil, and in these edges the interface among cathode, separator and anode films doesn't move during electrochemical process, as indicated by dashed circles; while for the rest part of the Jelly-Roll away from the constrained winding edges, the electrode film displays a buckling behavior with a periodic wavy-like profile, which resulted in the formation of several gaps/voids between electrode films as indicated by arrows.

In commercial pouch cell, the Jelly-Roll is sealed in the Al packing foil, its side edges are confined. According to the general mechanics theory, a buckling phenomenon is likely to be activated in some part of the Jelly-Roll without constraint when the lithiation induced stress in anode film develops to a critical level. And the actual wavy profile of the buckled electrode depends on the intrinsic stress level in graphite particle, the native mechanical constitutive of electrode film, and the extrinsic constraints/loads applied to the side edges of the Jelly-Roll.

Despite the cosmetic failure in rippled pouch cell, the expanded void/gap in Jelly-Roll needs to be filled with electrolyte, which causes the shortage of electrolyte in pouch cell for transportation of lithium ion between cathode and anode, and leads to the fast diving of cell capacity during cycle life test.

To suppress the void generation in pouch cell, the mechanical properties of the anode film can be enhanced through the application of stronger binders to retard the happening of buckling phenomenon, and relaxing the constraint on the side edges of the Jelly-Roll through stress control during the assembly of the Jelly-Roll can provide another choice for releasing the stress originated from lithiation.

4. Conclusion

In conclusion, an applicable method is applied to analyze the anode swelling induced by electrochemical process through selective blocking the transportation of lithium ion. Physical swelling and electrochemical swelling show different trends as a function of the electrochemical process. The stress evolution among the crystalline lattice expansion, the anode swelling and the rippling of the pouch cell is traced, where microscopic stress rooted from the intercalation of lithium ion into graphite lattice, is modified and magnified to a directional stress as mesoscopic anode swelling due to the confinement of Cu foil, and released through a visible buckling process finally. To avoid the rippling of the commercial pouch cell, optimized design of anode films with high mechanical strength are important, and the controllable stress during assembling and packing process can also play roles to modify the distribution of stress and constraint on Jelly-Roll.

References

[1] B.J. Hwang, Y.W. Tsai, D. Carlier, G. Ceder, Chem. Mater. 15 (2003) 3676–3682.
[2] Yukinori Koyama, Yoshinari Makimura, Isao Tanaka, Hirohiko Adachi, Tsutomu Ohzuku, J. Electrochem. Soc. 151 (2004) A1499–A1506.
[3] Daisuke Endo, Miki Yasutomi, Yoshihiro Katayama, Toshiyuki Nukuda, US Patent Pub. No. 20100233542A1, 2010.
[4] B.R. Lee, H.J. Noh, S.T. Myung, K. Amine, Y.K. Sun, J. Electrochem. Soc. 158 (2011) A180–A186.
[5] Won-Sub Yoon, Steven Iannopollo, Clare P. Grey, Dany Carlier, John Gorman, John Reed, Gerbrand Ceder, Electrochem. Solid-State Lett. 7 (2004) A167–A171.
[6] U. Kasavajjula, C. Wang, A.J. Appleby, J. Power Sources 163 (2007) 1003–1039.
[7] A. Magasinski, P. Dixon, B. Hertzberg, A. Kvit, J. Ayala, G. Yushin, Nat. Mater. 9 (2010) 353–358.
[8] D. Aurbach, B. Markovsky, I. Weissman, E. Leiv, Y. Ein-Eli, Electrochim. Acta 45 (1999) 67–86.
[9] J. Christensen, J. Newman, J. Solid State Electrochem. 10 (2006) 293–319.
[10] J. Christensen, J. Newman, J. Electrochem. Soc. 153 (2006) A1019–A1030.
[11] Stephen J. Harris, Rutooj D. Deshpande, Yue Qi, Indrajit Dutta, Yang-Tse Cheng, J. Mater. Res. 25 (2010) 1433–1440.